ECCOMAS Congress 2016
VII European Congress on Computational Methods in Applied Sciences and Engineering
M. Papadrakakis, V. Papadopoulos, G. Stefanou, V. Plevris (eds.)
Crete Island, Greece, 5–10 June 2016

TOPOLOGY OPTIMIZATION FOR FLUID FLOW EMPLOYING LOCAL OPTIMALITY CRITERIA

P. Sarstedt, G. Kachel, J. Ettrich, and K. Bühler

Hochschule Offenburg
University of Applied Sciences
Badstraße 24, D-77652 Offenburg, Germany
e-mail: philip.sarstedt@hs-offenburg.de

Keywords: Topology optimization, Local optimality criterion, Fluid flow, Navier-Stokes

Abstract. *We herein present a topology design method based on local optimality criteria which has been implemented in an open source Navier-Stokes solver for turbulent flows. Our method aims for the fast generation of geometry proposals in the early conceptual phase. To the best of our knowledge, this is the first local criteria approach utilizing a wall function turbulence model in order to consider turbulent flows. In order to allow for the growth as well as the shrinkage, or even the formation or disappearance of structural features, a topological approach is chosen. By introducing a volume fraction parameter, we distinguish between fluid and solid properties in each control volume. The fluid-solid interface is represented by an immersed boundary method using a piecewise linear surface reconstruction.*

1 INTRODUCTION

The development of fluid flow components, reaching from simple pipe systems to complex geometries, is still a challenging task for engineers and scientists. Usually a compromise between different design goals has to be made. Here CFD simulations coupled with optimization strategies are a valuable tool, but today they still go along with high computational costs. In order to keep these costs low and allow for a fast generation of geometry proposals in the early conceptual phase, we present a method based on local optimality criteria.

The term "optimization" is defined as the determination of design variables that minimize (or maximize) a cost (or objective) function with respect to a state equation possibly subject to constraints. This task can be accomplished by different strategies, for example classical gradient-based methods or Evolutionary Algorithms (EA). The former are fast but lack robustness and show the tendency to fall into local optima. Here recent progress is made in the calculation of the response sensitivities by the adjoint method which outperforms traditional methods like finite differences and has gained currency in commercial CFD software. Evolutionary Algorithms on the other hand are more robust but also computationally more expensive [15]. An example for an EA is the Generic Algorithm (GA) which mimics biological evolution. A third strategy, which is the subject of this paper and sometimes referred to as "bionic optimization", is based on local optimality criteria. Strictly speaking this method performs no optimization in the former defined sense, as a global extremal solution is not ensured. As we aim for a fast generation of appropriate geometry proposals rather than the optimal geometry, this is not considered necessary.

Furthermore we have to distinguish between *shape* and *topology* optimization. Shape optimization considers the parameterized bounding surface of the geometry. Topology optimization on the other hand utilizes all computational elements in a defined design space. This allows for the appearance of new boundaries and results in a much wider spectrum of possible solutions.

Shape optimization has been subject to research in the field of CFD since several decades, mainly in the sector of aeronautical problems, e.g. [13]. Well established in structural mechanics, topology optimization on the other hand is relatively new to CFD. The transfer of topology optimization from structural mechanics to computational fluid dynamics began with the work of Borrvall and Petersson in 2003 [2]. In their paper they considered the minimization of pressure drop in Stokes flow. In order to account for topological change, they adopted a source term of inverse permeability in the Stokes equation. In 2004 Moos et al. [11] presented a bionic topology optimization approach based on a local "backflow" criterion under the axiom that a fluid flow finds the best path under given constraints by itself. The method used the physical information of the flow field to deposit so called "virtual sand" in cells identified by the criterion. This local approach led to an improvement of the duct geometry within a very short computational period of time. Othmer et al. [12] picked up the idea of a backflow criterion in order to compute sensitivities for a climate channel optimization. Recirculation was detected by comparison of the actual velocity vector in a control volume with the potential flow solution. They implemented the optimization as a one-shot method in the CFD solver, which means that the optimization takes place in every iteration. The method was tested in 2D and 3D and characterized as extremely fast as regions with recirculation were inhibited that would usually require additional computing time. Recent effort was done by Wang et al. [16] who implemented a topology optimization method based on local optimality criteria in a lattice Boltzmann (LBM) framework. Prior to our investigations a project was carried out at Hochschule Offenburg by Gottlieb [6] which focused on the topological optimization of turbulent flows around blunt bodies. A method employing the backflow criterion for the recirculation region "behind" the body and a criterion of homogenization of gradients for the front part was developed. In contrast, our work focuses on internal flows which are viscous-dominated, whereas blunt bodies are dominated by pressure drag.

2 NUMERICAL METHODS

2.1 Governing equations

The governing equations express mass and momentum conservation. Steady viscous incompressible flows without volume forces can be described by the following set of equations, namely continuity and Navier-Stokes momentum equations

$$\nabla \cdot \mathbf{u} = 0, \tag{1}$$

$$(\mathbf{u} \cdot \nabla)\mathbf{u} = \nu \Delta \mathbf{u} - \frac{1}{\rho} \nabla p. \tag{2}$$

For turbulent flows, according to the Boussinesq hypotheses, the kinematic viscosity ν composes of two terms, the molecular and the turbulent kinematic viscosity $\nu = \nu_l + \nu_t$. Herein, the turbulent viscosity is calculated by a turbulence model. In industrial applications two-equation models like the k-ϵ or k-ω-SST model are state of the art for Reynolds-averaged Navier-Stokes (RANS) simulations.

2.2 Local optimality criteria

The idea behind local optimality criteria is the utilization of heuristic correlations between local flow parameters and their global impact. In this way the calculation of sensitivities with respect to a global cost function is circumvented. In this section different optimality criteria are presented.

Following the idea of Moos et al. [11] we implement a backflow criterion. In order to avoid losses caused by recirculation, such regions are identified and set to solid. Therefore a comparison of the local velocity vector with a reference vector can be performed. If a specified angle of deviation, e.g. 90 degrees, is exceeded, backflow is present. The angle of deviation λ is calculated from the scalar product of the actual velocity vector $\mathbf{u}$ and a reference vector $\mathbf{u}_{ref}$ as follows:

$$\lambda = \frac{\mathbf{u}}{|\mathbf{u}|} \cdot \frac{\mathbf{u}_{ref}}{|\mathbf{u}_{ref}|}. \tag{3}$$

The reference vector can be obtained through different approaches. In a straight channel the direction from inlet to outlet is a sensible choice for $\mathbf{u}_{ref}$. In complex flow domains the potential flow field is a fast way to obtain a sensible reference vector field, as it contains no backflow regions by definition.

Wang et. al [16] proposed a different optimality criterion algorithm based on the natural behavior of erosion and deposition of sand in river basins. They introduced two local optimality criteria: At the fluid-solid interface, vanishing solid cells are chosen by maximum wall shear stress

$$\tau_w = \mu \left(\frac{\partial u}{\partial y} \right)_w, \tag{4}$$

with the dynamic viscosity μ. On the other hand solidifying fluid cells are chosen by lowest dynamic pressure

$$p_{dyn} = \frac{\rho}{2} |\mathbf{u}|^{\mathbf{2}}. \tag{5}$$

Based on the work of Bourot [3] we derive another criterion based on the homogenization of gradients. Bourot observed a correlation between vorticity and optimal body shapes in Stokes flow. A homogenization of the vorticity magnitude on the surface of the body led to optimal shapes with respect to flow loss. The vorticity is defined as the curl of the velocity vector (cf. Eq. (6)) and can be interpreted as a measure of the rate of rotation of a fluid element [9].

$$\omega = \nabla \times \mathbf{u}. \tag{6}$$

An often encountered issue in flow optimization is the relocation of loss inducing geometrical features to the proximity of the outlet. This results in a seemingly reduced loss inside the considered domain as the loss takes place behind the outlet. An example would be a sharp edge at the outlet of the design space resulting in a flow separation in the adjacent pipe. In order to avoid such a behavior, we introduce an adaption region (AR) for the inlet and outlet, cf. figure 1. Herein the adapted reference vectors are obtained by interpolation between the reference vector field $\mathbf{u}_{ref}$ and the boundary normal vector (e.g. $\mathbf{u}_{ref_{out}}$). In addition we limit the angle of deviation λ more strictly as we approach the boundary. Also a *fixed* fluid region in the vicinity of the inlet and outlet is introduced where no geometrical change is performed by the optimization algorithm. For this purpose the inverse permeability coefficient α is fixed to zero. Altogether this leads to an almost orthogonal outflow and the prevention of outlet blockage.

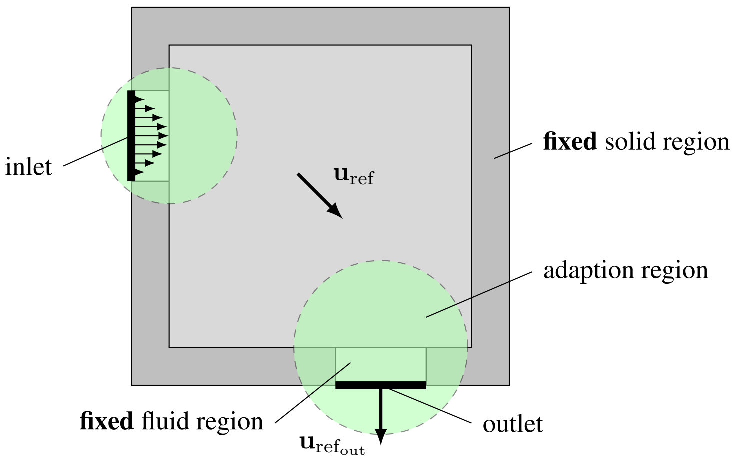

Figure 1: Adaption regions and fixed regions.

2.3 Optimization algorithm

As discussed earlier, we utilize a topology optimization with all control volumes serving as parameters. In order to distinguish between fluid and solid cells, we introduce the scalar volume fraction field Ψ, defining the ratio of the cell-volume occupied by solid to the total cell-volume:

$$\Psi = \frac{V_{solid}}{V_{total}}. \tag{7}$$

The volume fraction serves as the parameter for the optimization algorithm and is manipulated according to the method of steepest descent with a constant step size δ.

$$\Psi_{new} = \Psi_{old} - \delta\lambda. \tag{8}$$

Basically this is done in a “one-shot” fashion for every timestep [12].

3 TOPOLOGY REPRESENTATION

The representation of topological features of a time dependent flow domain is subject of this section. In the literature different approaches are found that can be classified into two categories: *Mesh morphing (MM)* and *immersed boundary methods (IBM)*. In mesh morphing a body fitted computational grid is distorted according to the displacement of the boundary. In immersed boundary methods the simulation is carried out on a Cartesian grid where the effect of the boundary is imposed on the flow through a source term in the governing equations. For an extensive overview of the different IBM methods we refer the reader to Mittal and Iaccarino [10]. As we aim for a fast optimization method a recomputation of the mesh for each iteration is too cost intensive. Therefore, following the work of Angot et al. [1] and Khadra et al. [8], we assume the design space as a porous medium and the flow to be governed by the Navier-Stokes/Brinkman equations, also called penalized Navier-Stokes equations [4] or penalization method (PM) [5]. For a steady viscous incompressible flow the equations read

$$(\mathbf{u} \cdot \nabla)\mathbf{u} = \nu \Delta \mathbf{u} - \alpha \mathbf{u} - \frac{1}{\rho} \nabla p, \tag{9}$$

with the inverse permeability coefficient α. If $\alpha = 0$, the Navier-Stokes equations are solved and the flow is a fully liquid phase. If α tends to infinity, the medium is solid and the equations tend to the Darcy equation. For numerical reasons α is set to $\alpha_{max} = 10^5$ in the solid domain. This approach can be seen as an immersed boundary method with the main advantage that an imposition of a boundary condition at the fluid-solid interface is not necessary. For laminar flows it appropriately mimics the effects of solid boundaries on the flow as will be shown in the subsequent section.

In order to account for the technically important fields of application, the topology representation approach has to be capable of considering highly turbulent flows. Here the boundary layer at walls is critical for the accuracy of the simulation as it contains large gradients of the flow quantities. In RANS simulations a very fine mesh to the wall is generally used in order to resolve these gradients sufficiently. This approach is known as low Reynolds number approach (Low-Re). It is not suitable for a fast topology optimization as the position of the walls is not known a priori and the mesh would have to be very fine everywhere or refined around the boundaries for every change in topology. In order to circumvent such an excessive grid resolution, a high Reynolds number turbulence model approach (High-Re), also called wall function approach, can be used to skip the boundary layer via a universally valid wall function.

In simulations with high Reynolds number flow the Navier-Stokes/Brinkman approach leads to large errors in the flow field prediction, caused by the step-wise representation of the fluid-solid interface and a missing treatment of the turbulent quantities. This affects the optimization and leads to unrealistic geometry proposals. Therefore a more advanced immersed boundary method is used to guarantee proper fluid-solid interface treatment. Here, the discrete forcing approach with direct imposition of boundary conditions is the most promising [10]. By modification of the discretized equations near the fluid-solid interface, the immersed boundary acts like a body fitted mesh. This leads to a higher accuracy which is critical for high Reynolds number flows. Such an IBM was recently implemented in the OpenFOAM Extend Project [7].

Currently we are working on the adaption of the immersed boundary method to handle moving and deforming boundaries. The idea is, that the optimization algorithm still manipulates the volume fraction field Ψ according to the local optimality criteria, where Ψ is used to extract the geometry through a linear surface reconstruction [14]. The resulting surface geometry data is then fed to the immersed boundary method. As this procedure is more cost intensive, it is no longer coupled to the solver in a "one-shot" fashion but performed at a defined time step interval. A drawback in terms of topology optimization is the exclusion of the solid region from the solution. Once blocked out, the removal of solid cells is only possible at the fluid-solid interface. Here criteria like magnitude of shear stress or vorticity are applicable. Therefore the method can be classified partly as topology and partly as shape optimization.

4 NUMERICAL EXAMPLES

4.1 Plane channel

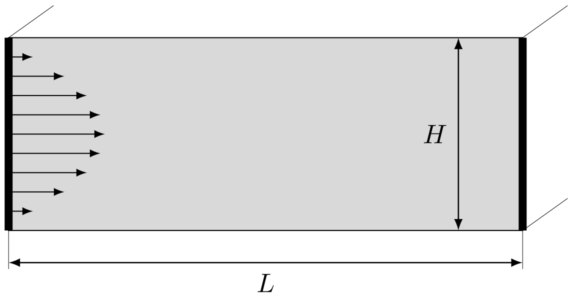

Figure 2: Dimensions of the "plane channel" simulation domain.

To show the validity of the penalization method as well as the immersed boundary method with discrete forcing approach and direct imposition of boundary conditions, we consider a 2D steady viscous incompressible channel flow. In order to achieve a fully developed flow, a periodic boundary condition is applied, which maps the flow quantities from the outlet to the inlet. For a laminar flow at $Re = 40$ the solution calculated with a body fitted mesh (BF) matches the analytical solution. In order to apply the penalization method, an additional layer of control volumes is added to the top and bottom of the flow domain. Here the inverse permeability coefficient α is set to 10^5, driving the velocity towards zero in the cell centers. This does not exactly enforce the no-slip boundary condition at the cell faces which leads to an artificially increased channel height and a lower maximum velocity, cf. figure 3a. For a turbulent flow at $Re = 25,000$ the penalization method shows an artificially increased boundary layer thickness, cf. figure 3b. This originates from the missing treatment of the turbulent quantities at the fluid-solid interface. The immersed boundary method however shows a much better agreement with the body fitted mesh solution, since the boundary condition is applied sharply at the fluid-solid interface and the turbulence is treated by a wall function approach through a high Reynolds number turbulence model. This study suggests the adoption of the immersed boundary method with discrete forcing approach and direct imposition of boundary conditions for the optimization of turbulent flows. The implementation is still under development at the moment and will be presented in subsequent publications.

4.2 Right angle elbow

In order to demonstrate the optimization method, a 2D rectangular simulation domain with a velocity inlet on the upper left boundary and a zero-pressure outlet on the lower right boundary is considered, cf. figure 4. At the inlet and outlet no-adaption zones are applied. The inner rectangular domain represents the so called design space and is bounded by a solid region, enforced by the penalization method with $\alpha = 10^5$. For the numerical calculations the design space is divided into 200×200 unit square cells, forming an equidistant Cartesian grid. The

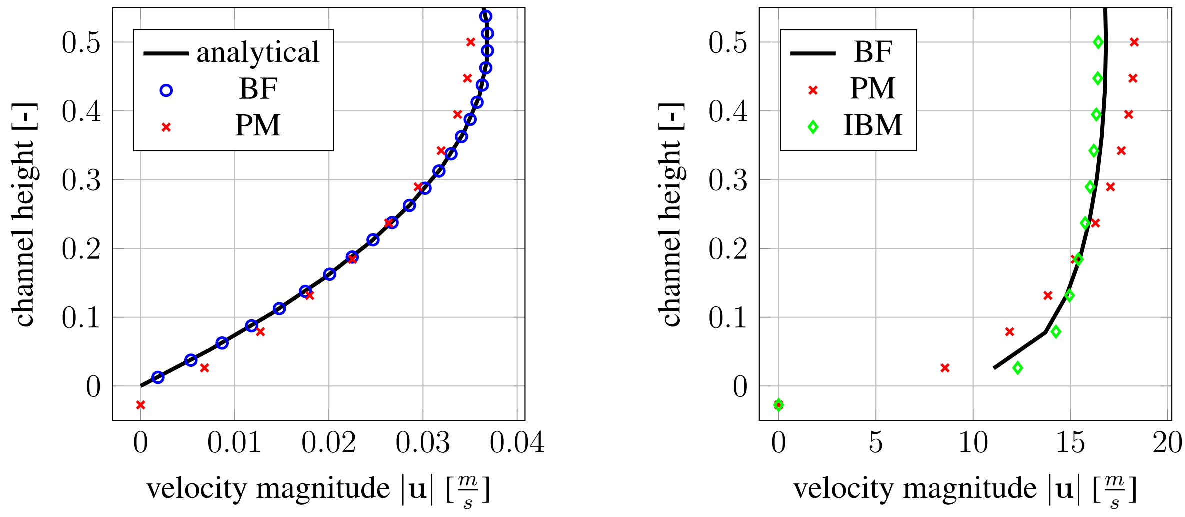

(a) $Re = 40$

(b) $Re = 25,000$

Figure 3: Comparison of velocity profiles obtained with body fitted mesh (BF), penalization method (PM) and immersed boundary method (IBM) for laminar and turbulent flows.

fluid is assumed as air with a kinematic viscosity of $\nu = 1.56 \times 10^{-5} \frac{m^2}{s}$. Depending on the inlet length $L_{in} = 0.2L$ with $L = 0.05m$ the mean inlet velocity $\overline{u}_{in}$ is adjusted to match the desired Reynolds number $Re = \frac{L_{in}\overline{u}_{in}}{\nu}$. In order to assess the geometry proposed by the optimization methods, the total pressure loss $\Delta\tilde{p}_t$ is calculated from the mass flow averaged total pressures $\tilde{p}_t$ at inlet and outlet.

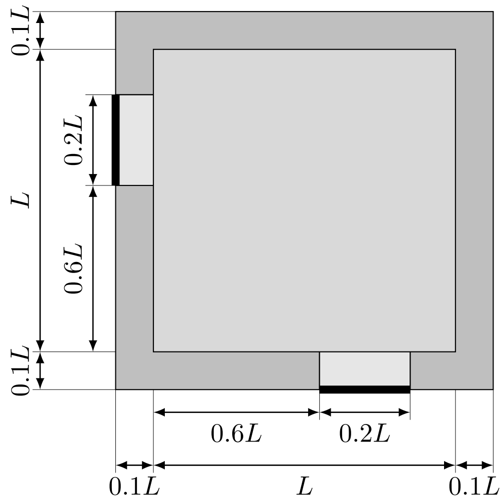

Figure 4: Dimensions of the “right angle elbow” simulation domain.

We consider the laminar case where the fully developed flow enters the domain at a Reynolds number of $Re = 40$. The steady-state solution of the flow shows two recirculation regions in the upper right and lower left corner of the design domain, cf. figure 5a. These regions are undesirable as they cause losses, therefore the aim is to generate a geometry that leads to no such regions. Figure 5b shows the solution of the optimization based on the backflow criterion. In this case the potential flow, represented as white colored streamlines, was used as reference vector field. As the simulation progresses the recirculation regions are blocked by the penalization method, resulting in an improved total pressure loss of 93.34%.

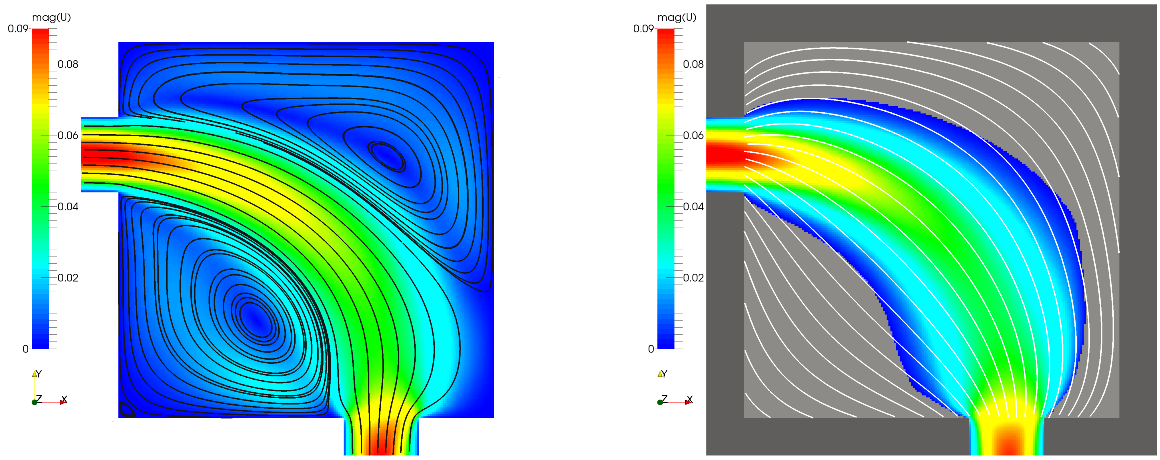

(a) BF mesh, no optimization

(b) PM, backflow optimization

Figure 5: Bionic optimization of a right angle elbow with the potential flow solution used as reference vector field for the backflow criterion ($Re = 40$).

In order to demonstrate the functionality of the adaption regions, an optimization case of the right angle elbow with a reference vector set to $\mathbf{u}_{ref} = (1, -1, 0)$ is considered, cf. streamlines in Fig. 6d. Figure 6 shows the obtained geometry proposals. The reference vector as well as the allowed angle of deviation λ is manipulated inside the adaption regions through interpolation. The aim is a geometry proposal that leads to an orthogonal outflow at the outlet. If this is not the case the proposed solution can not be considered as a proper one as it would lead to recirculation regions behind the outlet. Figure 7 shows the velocity components u and v at the outlet. The increased x-velocity u indicates that the geometry obtained without adaption regions has a higher probability of forming recirculation regions behind the outlet. The cases with adaption regions show a reduction of the x-velocity depending on the adaption region parameters.

Besides velocity vectors, other flow quantities can be considered as local optimization criteria. The shear stress as well as the vorticity criterion are examples for criteria that are applicable at the fluid-solid interface. Here the optimization algorithm checks for the highest absolute values of the respective quantity and gradually converts the near solid cells to fluid cells, leading to a homogenization of gradients. To demonstrate this functionality, a sharp 90 degree bend is used as initial geometry, cf. figure 8a. Figure 8 shows two geometry proposals obtained by the shear stress criterion and the vorticity criterion. The sharp corners of the initial solution were smoothed and the channel width has increased, leading to a reduced total pressure loss of 51.21% for the shear stress criterion and 37.68% for the vorticity criterion, cf. figure 9.

An advantage of the penalization method is its seamless extension to 3D cases without additional modification. Figure 10 shows examples of 3D flow optimization with the backflow criterion. The first case is a flow around a circular disc inside a rectangular channel at a Reynolds number of $Re = 800$. Through the deposition of solid cells in front of as well as behind the circular disc, flow separation is avoided, leading to a more aerodynamic shape. The second case shows a turbulent flow at $Re = 20,000$ through a rectangular channel with a cavity. Although we know that the penalization method lacks the correct treatment of the turbulence quantities at the fluid-solid interface, the solution can be considered as an improvement as the geometry is

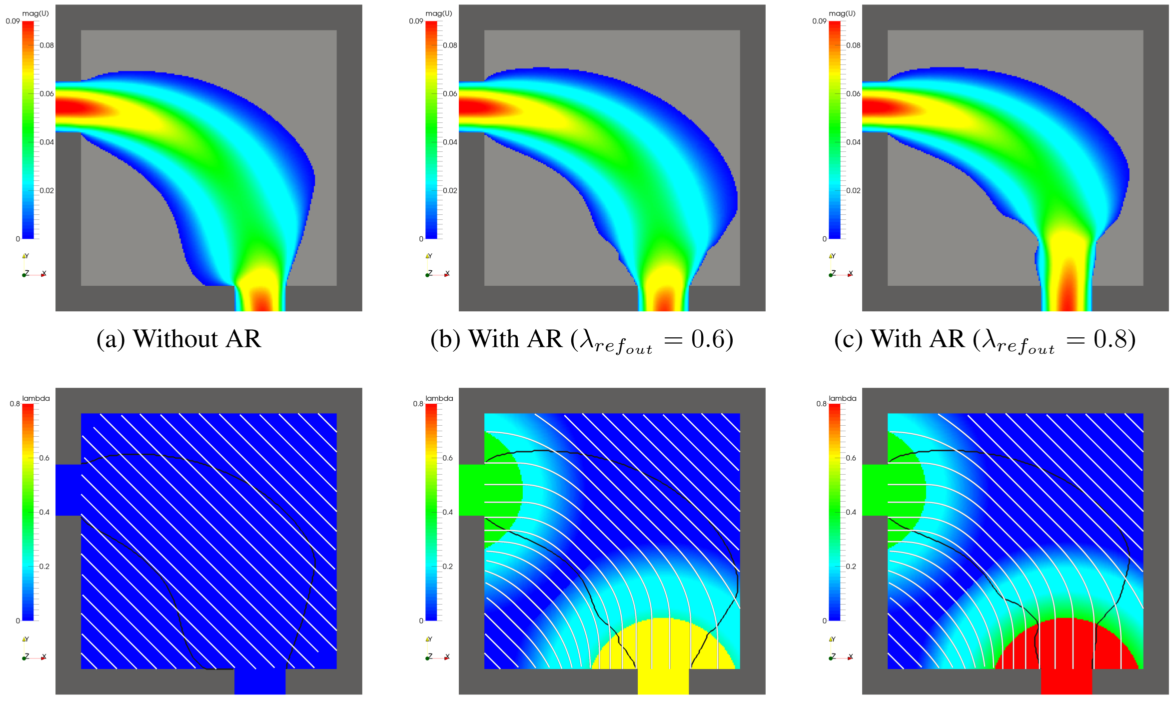

(a) Without AR (b) With AR ($\lambda_{ref_{out}} = 0.6$) (c) With AR ($\lambda_{ref_{out}} = 0.8$)

(d) Without AR (e) With AR ($\lambda_{ref_{out}} = 0.6$) (f) With AR ($\lambda_{ref_{out}} = 0.8$)

Figure 6: Velocity field of three different bionic optimizations of a right angle elbow at $Re = 40$ without (a) and with adaption regions (b, c). Streamlines of the reference vector field $\mathbf{u}_{ref}$ and the angle of deviation λ (d, e, f).

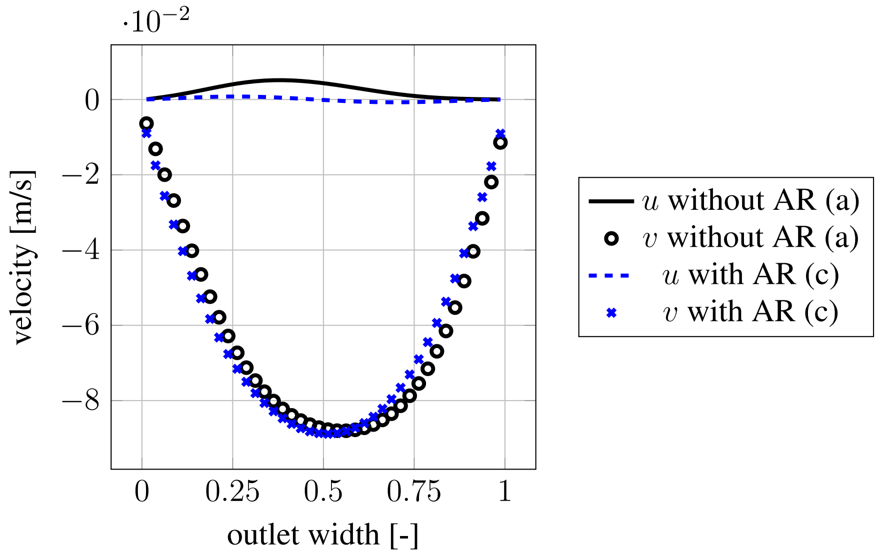

Figure 7: Velocity component u and v at the outlet of case 6a without and case 6c with adaption regions.

smoothed, reducing the likeliness of flow separation.

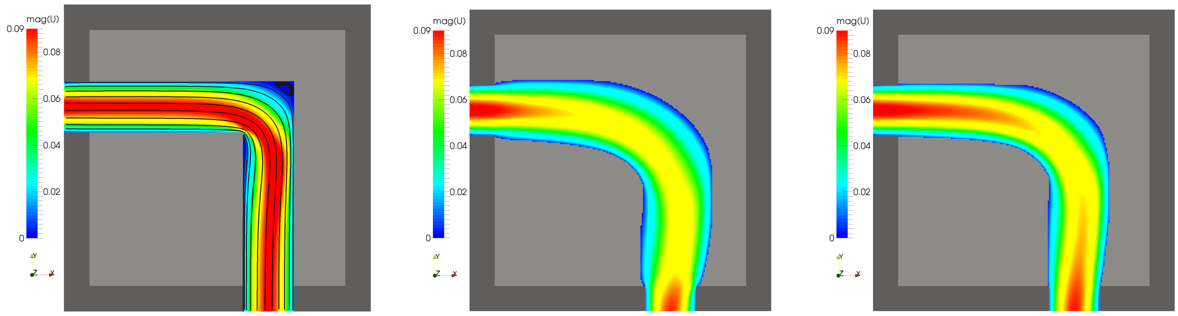

(a) No optimization (b) Shear stress crit. (c) Vorticity crit.

Figure 8: Bionic optimization of a sharp 90 degree bend ($Re = 40$).

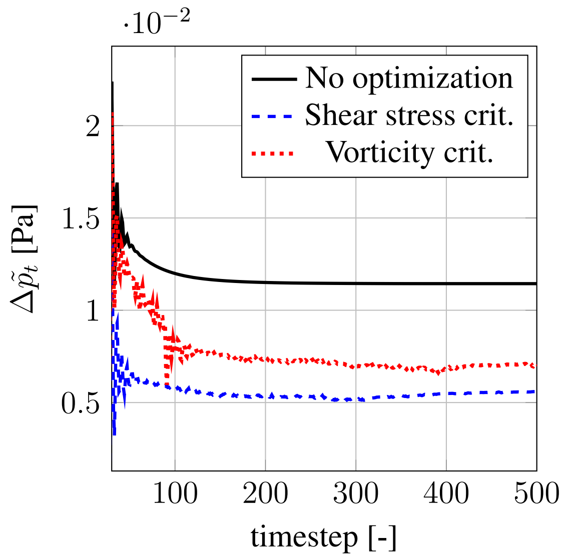

Figure 9: Mass flow averaged total pressure loss over timesteps for a sharp 90 degree bend ($Re = 40$).

5 DISCUSSION AND OUTLOOK

A design method that aims for the fast generation of appropriate geometry proposals in the early conceptual phase based on local optimality criteria was presented for the Finite-Volume Navier-Stokes CFD software OpenFOAM. Several criteria based on backflow, shear stress and vorticity magnitude, were implemented and investigated. Furthermore a method working with adaption regions was proposed in order to avoid recirculation regions behind the outlet. It was shown that hereby the velocity component perpendicular to the outlet normal vector can be reduced in the outlet plane. In order to realize a fast way of adapting the boundary during the simulation, a penalization method was adopted and its applicability successfully shown for 2D and 3D cases. Numerical examples were presented for a 2D right angle elbow at Reynolds number $Re = 40$, a circular disk in a 3D channel at $Re = 800$ and a 3D channel with cavity at $Re = 20,000$. For turbulent flows an immersed boundary method with discrete forcing approach and direct imposition of boundary conditions was adopted in order to consider correctly the turbulent quantities at the boundary. A 2D channel flow at $Re = 25,000$ calculated with this immersed boundary method shows a good agreement with the body fitted mesh solution. The integration of the immersed boundary method into the optimization algorithm is still under progress and results will be shown in subsequent publications. Future efforts will focus on

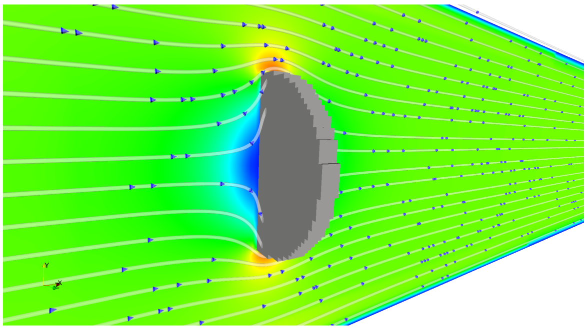

(a) Circular disk in a 3D channel

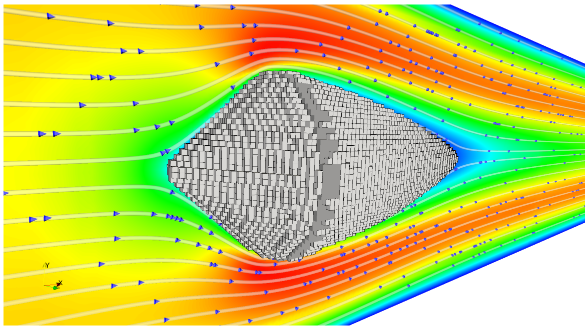

(b) Optimized circular disc ($Re = 800$)

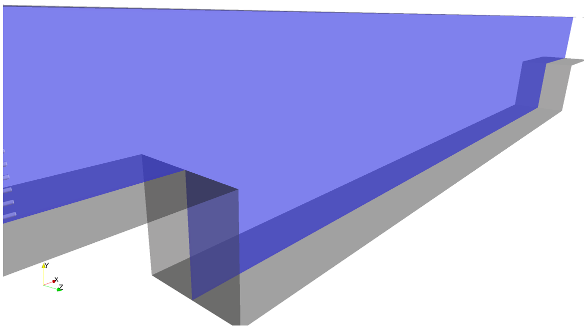

(c) 3D channel with cavity

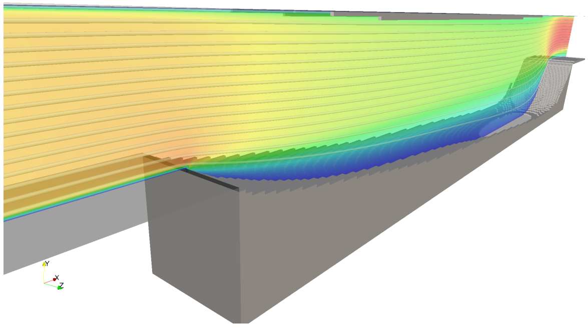

(d) Optimized cavity ($Re = 20,000$)

Figure 10: Examples of 3D bionic optimization.

the final implementation of the immersed boundary method to handle moving and deforming boundaries as this is vital for the correct treatment of turbulent flows. Furthermore the development of the optimization method with the main focus on the definition and evaluation of further optimality criteria is planned.

ACKNOWLEDGEMENT

The reported work was carried out as part of the FHprofUnt founding project, project number FKZ 03FH037PA2 (FoEn). The authors greatly acknowledge the financial support provided by the Federal Ministry of Education and Research (BMBF).

REFERENCES

[1] P. Angot, C.H. Bruneau, P. Fabrie, A penalization method to take into account obstacles in incompressible viscous flows. *Numerische Mathematik*, **81**, 497–520, 1999.

[2] T. Borrvall, J. Petersson, Topology optimization of fluids in Stokes flow. *International Journal for Numerical Methods in Fluids*, **41**, 77–107, 2003.

[3] J.M. Bourot, On the numerical computation of the optimum profile in Stokes flow. *Journal of Fluid Mechanics*, **65**, 513–515, 1974.

[4] H.C. Brinkman, A calculation of the viscous force exerted by a flowing fluid on a dense swarm of particles. *Applied Scientific Research*, **1**, 27–34, 1947.

[5] C.H. Bruneau, I. Mortazavi, Numerical modelling and passive flow control using porous media. *Computers & Fluids*, **37**, 488–498, 2008.

[6] A. Gottlieb, Vorauslegung umströmter Bauteile durch Anwendung lokaler Optimalitätskriterien. PhD thesis, Universität Stuttgart, 2013.

[7] H. Jasak, D. Rigler, Ž. Tuković, Finite volume immersed boundary method for turbulent flow simulations. *9th OpenFOAM Workshop*, Zagreb, 2014.

[8] K. Khadra, P. Angot, S. Parneix, J.P. Caltagirone, Fictitious domain approach for numerical modelling of Navier-Stokes equations. *International Journal for Numerical Methods in Fluids*, **34**, 651–684, 2000.

[9] H.J. Lugt, *Introduction to Vortex Theory*, Vortex Flow Press, Potomac, MD, 1996.

[10] R. Mittal, G. Iaccarino, Immersed Boundary Methods. *Annual Review of Fluid Mechanics*, **37**, 239–261, 2005.

[11] O. Moos, F.R. Klimetzek, R. Rossmann, Bionic Optimization of Air-Guiding Systems. *SAE Technical Paper 2004-01-1377*, 2004.

[12] C. Othmer, T. Kaminski, R. Giering, Computation of topological sensitivities in fluid dynamics: Cost function versatility. *ECCOMAS CFD*, Delft, 2006.

[13] O. Pironneau, On Optimal Design in Stokes Flow. *Journal of Fluid Mechanics*, **59**, 117–128, 1973.

[14] R. Scardovelli, S. Zaleski, Analytical Relations Connecting Linear Interfaces and Volume Fractions in Rectangular Grids. *Journal of Computational Physics*, **164**, 228–237, 2000.

[15] D. Thévenin, G. Janiga, *Optimization and Computational Fluid Dynamics*, Springer, Berlin, Heidelberg, 2008.

[16] L. Wang, Y. Fan, L. Luo, Heuristic optimality criterion algorithm for shape design of fluid flow. *Journal of Computational Physics*, **229**, 8031–8044, 2010.